AECL-8180

ATOMIC ENERGY OF CANADA LIMITED

L'ÉNERGIE ATOMIQUE DU CANADA LIMITÉE

COMPUTATION OF TWO-DIMENSIONAL ISOTHERMAL FLOW IN SHELL-AND-TUBE HEAT EXCHANGERS

Calcul des écoulements bidimensionnels et isothermiques dans les échangeurs thermiques à tubes et enveloppes

L.N. CARLUCCI, P.F. GALPIN, J.D. BROWN and V. FRISINA

Paper presented at the 1983 HTFS Research Symposium, Bath, United Kingdom

Chalk River Nuclear Laboratories Laboratoires nucléaires de Chalk River

Chalk River, Ontario

July 1983 juillet

COMPUTATION OF TWO-DIMENSIONAL ISOTHERMAL FLOW IN SHELL-AND-TUBE HEAT EXCHANGERS

L.N. Carlucci, P.F. Galpin, J.D. Brown, V. Frisina

Presented at the 1983 HTFS Research Symposium

Bath, United Kingdom

Chalk River Nuclear Laboratories

Chalk River, Ontario, K0J 1J0

1983 July

AECL-8180

L'ENERGIE ATOMIQUE DU CANADA, LIMITEE

Calcul des écoulements bidimensionnels et isothermiques dans les échangeurs thermiques à tubes et enveloppes

par

L.N. Carlucci, P.F. Galpin, J.D. Brown et V. Frisina

Résumé

On décrit une méthode permettant de calculer la répartition des écoulements bidimensionnels, isothermiques, du côté enveloppe dans des grappes de tubes ayant des limites arbitraires et des dispositifs de blocage des écoulements, tels que des bandes de scellement, définis dans des emplacements arbitraires. Cette méthode est décrite de façon assez détaillée et plusieurs résultats calculés sont présentés pour illustrer sa robustesse et son caractère général.

Laboratoires nucléaires de Chalk River
Chalk River (Ontario) K0J 1J0

Juillet 1983

AECL-8180

COMPUTATION OF TWO-DIMENSIONAL ISOTHERMAL FLOW IN SHELL-AND-TUBE HEAT EXCHANGERS

L.N. Carlucci, P.F. Galpin, J.D. Brown, V. Frigina

Atomic Energy of Canada Limited
Chalk River Nuclear Laboratories
CHALK RIVER, Ontario KOJ 1JO

ABSTRACT

A computational procedure is outlined whereby two-dimensional isothermal shell-side flow distributions can be calculated for tube bundles having arbitrary boundaries and flow blocking devices, such as sealing strips, defined in arbitrary locations. The procedure is described in some detail and several computed results are presented to illustrate the robustness and generality of the method.

NOMENCLATURE

A	Flow area
a	Convection-diffusion coefficient in finite control volume equation
C_t	Coefficient in equation (7) equal to: 1 for square and triangular; $\sqrt{3/2}$ for rotated triangular and $1/\sqrt{2}$ for rotated square tube layouts
d	Tube diameter
F	Fraction of control volume filled with tubes
f	Friction factor
h	Metric coefficient equals to: 1 for cartesian and y for polar coordinates
I,J	Grid in x and y direction
k	Loss coefficient
P, P'	Pressure and pressure correction
PSS1, etc	Cartesian coordinates of flow blocking device
P	Tube pitch
S	Source term in equations (1) and (2)
s	Distance between tube rows along flow direction
sc	Distance between close approaches
Su	Source term in finite control volume equation
SS1, etc	Length of segments of flow blocking device
u,v	Velocity in x and y direction
x	Coordinate: linear in cartesian and angular in polar
y	Linear coordinate
Z0	Coordinates of bundle corner
β	Local volume porosity = fluid volume ÷ total volume
$\Delta P/\Delta L$	Frictional pressure gradient
Δy	Incremental distance along y
μ	Dynamic viscosity
ρ	Density
ϕ	General transport parameter in finite control volume equation, stands for u, v or P'

Subscripts

b	Bypass or tube-free region
bl	Flow blockage device
cv	Control volume
eff	Effective
fs	Free-stream
g, gap	Local and overall gap of flow blockage device
max	Maximum
min	Minimum
nb	Neighbouring point node
p	Main node point
sl	Shock loss

June 1983

t Tube-bundle or tube-filled region
u U-velocity
v V-velocity

1. INTRODUCTION

Stream analysis-based computer codes such as TASC are currently the most widely accepted tools available for the thermal-hydraulic rating of shell-and-tube heat exchangers. While such tools are sufficiently accurate for evaluating overall parameters such as heat duty and pressure drop, they are inadequate for estimating local shell-side flow conditions. However, robust numerical modelling methods exist which can be used to calculate the detailed shell-side flow and heat transfer with relative ease. These techniques are routinely used to analyze the thermal-hydraulics of nuclear steam generators [1-4].

A multi-dimensional description of the shell-side flow and heat transfer has several potential uses:

- calculating local velocities for flow-induced vibration analysis,
- identifying stagnant low heat transfer regions susceptible to fouling or corrosion,
- optimizing tube bundle and sealing strip layout to minimize bypass flow,
- optimizing the thermal-hydraulics of complex components such as power plant condensers, and
- developing refinements for stream analysis-based codes using results from "numerical" rather than laboratory experiments.

The accuracy of a multi-dimensional calculation depends not only on the empirical fluid-flow correlations used but also on how well internal obstructions such as tube bundles, sealing strips and baffles are described in the numerical model. To this end, procedures have been developed to accurately model tube bundles of arbitrary shape and flow blocking devices located anywhere in the modelled region. Once defined, porous media concepts, incorporated in the governing equations , are used to account for the anisotropic impedances and flow volume reductions due to these obstructions.

This paper presents an outline of the equations governing the two-dimensional flow of an isothermal fluid, the discretization and solution method used and the procedures developed to describe tube bundles having arbitrary boundaries and flow blocking devices at arbitrary locations. Several examples are presented to illustrate the robustness and generality of the modelling approach.

2. FLOW EQUATIONS

The equations governing the steady two-dimensional flow of an incompressible isothermal fluid in a porous medium are those of momentum and continuity. Assuming that the porous medium is adequately represented by an isotropic porosity distribution, these equations take on the following conservation forms which are valid in either polar (h=y) or cartesian (h=1) coordinates,

x-momentum:

$$\frac{1}{h}\frac{\partial}{\partial x}\left[\beta(\rho u^2 - \mu_{eff}\frac{\partial u}{h\partial x})\right] + \frac{1}{h}\frac{\partial}{\partial y}\left[h\beta(\rho uv - \mu_{eff}\frac{\partial u}{\partial y})\right] = \beta\left[S_u - \frac{1}{h}\frac{\partial P}{\partial x} - k_u\rho|u|u\right] \quad (1)$$

y-momentum:

$$\frac{1}{h}\frac{\partial}{\partial x}\left[\beta(\rho uv - \mu_{eff}\frac{\partial v}{h\partial x})\right] + \frac{1}{h}\frac{\partial}{\partial y}\left[h\beta(\rho v^2 - \mu_{eff}\frac{\partial v}{\partial y})\right] = \beta\left[S_v - \frac{\partial P}{\partial y} - k_v\rho|v|v\right] \quad (2)$$

continuity:

$$\frac{1}{h}\frac{\partial}{\partial x}(\beta\rho u) + \frac{1}{h}\frac{\partial}{\partial y}(h\beta\rho v) = 0 \quad (3)$$

The porosity, defined on a local basis as the ratio of fluid volume to total volume, accounts for the flow volume reduction of the tube bundle. It is assumed to be locally

isotropic so that if a control volume is entirely within a tube-filled region the corresponding surface permeabilities* and porosity are numerically equal and independent of direction. Thus, the porosity within a tube bundle laid out in a regular pattern is a constant calculated from the characteristic pitch and tube diameter. For instance, the porosity for a tube bundle laid out in a square or rotated square pattern is calculated from:

$$\beta_t = 1 - \frac{\pi}{4}\left(\frac{d}{p}\right)^2 \qquad (4)$$

while for a triangular or rotated triangular layout it is given by:

$$\beta_t = 1 - \frac{\pi}{2\sqrt{3}}\left(\frac{d}{p}\right)^2 \qquad (5)$$

While the porosity within a tube bundle is readily defined by these expressions, the porosity near the bundle boundaries is affected by the bundle shape. Definitions of the porosity distribution for bundles with arbitrary boundaries are given in Section 4.

The coefficients k_u and k_v in the momentum equations reflect the net local hydraulic flow resistance along each coordinate direction due to the tubes, bypass lanes and flow blockage devices. For example, a v-velocity control volume, that is partially blocked by a sealing strip and that includes a tube-filled as well as a tube-free region, has the following components in k_v:

$$k_v = k_{v,t} + k_{v,b} + k_{v,bl} \qquad (6)$$

where, the tube-bundle loss coefficient is given by:

$$k_{v,t} = 2\left(\frac{f_t}{s}\right)\left(\frac{C_t p \beta}{p-d}\right)^2\left[\frac{1-\beta}{1-\beta_t}\right] \qquad (7)$$

the bypass or tube-free loss coefficients is defined by:

$$k_{v,b} = 2\left(\frac{f_b}{sc}\right)\left[\frac{\beta-\beta_t}{1-\beta_t}\right] \qquad (8)$$

* Surface permeability = ratio of fluid area to total fluid-plus-solid area on a control volume face.

and the sealing strip loss coefficient is defined by:

$$k_{v,bl} = \begin{cases} \frac{k_{sl}}{2\Delta y}\left(\frac{A_{cv}}{A_g}\right)^2 ; & \frac{A_{cv}}{A_g} > 1 \\ \frac{k_{sl}}{2\Delta y} ; & 0 < \frac{A_{cv}}{A_g} \leq 1 \\ 10^{30} ; & A_g = 0 \end{cases} \qquad (9)$$

The square bracketed terms in equations (7) and (8) are weighting factors included to ensure that $k_{v,t}$ and $k_{v,b}$ approach zero as the volume fractions of the tube-filled and tube-free regions approach zero. The second round-bracketed term in equation (7) accounts for the fact that the tube-bundle friction factor f_t is based on the velocity across the smallest inter-tube gap* rather than the porosity-based velocity, v.

The "shock loss" coefficient k_{sl} in equation (9) is calculated assuming the gap between a flow blockage device and a tube or a shell wall has the same loss characteristics as an orifice having a representative ratio of approach area to gap area (Figure 1). It is important to note that $k_{v,bl}$ will have one of the three values calculated from equation (9) only when a flow blockage device and its effective gap cross the control volume of interest, otherwise it will be set to zero. The procedures for defining arbitrarily located blocking devices is described in Section 5.

* Butterworth [5] has successfully correlated a wide range of ideal tube-bundle data using the following definition for f_t:

$$f_t = \frac{\Delta P}{\Delta L}\left(\frac{d}{2\rho v_{fs}^2}\right)$$

The corresponding expression for $k_{v,t}$ is then given by:

$$k_{v,t} = 2\left(\frac{f_t}{d}\right)(\beta^2)\left[\frac{1-\beta}{1-\beta_t}\right]$$

The parameters S_u and S_v in equations (1) and (2) contain all left-over terms that do not fit the standard equation format. These include diffusion terms, and, if a polar co-ordinate system is used, centrifugal and Coriolis acceleration terms.

3. FINITE CONTROL VOLUME TREATMENT

The method of discretization and numerical solution procedure used are described in detail elsewhere [6,7]; only the main features are given here. First, the region to be modelled is subdivided into a number of control volumes defined on either a polar or cartesian co-ordinate grid. A staggered mesh is used so that three different control volumes are defined for a given node point, one for each of the vector variables and one for all scalar variables (Figure 2). Then, each of the transport equations is integrated over its own control volume. The convection-diffusion flux terms are approximated using the hybrid upwind/central discretization scheme. The linearized finite control volume analogue of each momentum equation that results for a control volume centered about p and surrounded by four neighbouring points nb, has the form:

$$a_p\phi_p = \sum_{nb} a_{nb}\phi_{nb} + Su \qquad (10)$$

The pressure-velocity coupling, or compressibility constraint, is handled by the SIMPLE* algorithm of Patankar and Spalding [6]. SIMPLE combines the momentum and continuity equations to form a Poisson-like pressure-correction equation which has the same form as (10). Once solved for, the pressure corrections are used to update both pressure and velocity fields such that continuity is satisfied.

The three algebraic equations are solved sequentially by iteration using multiple sweeps of the tridiagonal matrix line solver [6].

* SIMPLE - Semi-IMplicit Pressure-Linked Equations

4. POROSITY DISTRIBUTION

As already indicated, the effects of tube bundles of arbitrary shape are modelled in two ways: 1) by defining a volume-based porosity distribution which accounts for fluid volume reduction, and 2) by defining momentum sink terms which reflect the local hydraulic resistance of the individual tubes. It is obvious that to get a good estimate of the latter it is important to accurately define the former. This is clearly illustrated by equations (7) and (8) which show the role of β in determining the relative weights of the hydraulic resistances of tube-filled and bypass regions. The algorithm developed to define the porosity distribution can be described as follows:

1. From engineering drawings and specification sheets, determine the number of tube-bundle sections together with tube diameter, pitch and layout type.

2. For each bundle section in turn, define the coordinates of a suitable corner. Then, define each boundary segment by specifying the direction and number of centre-to-centre tube spacings along that direction. This step is illustrated in Figure 3 for a tube bundle having a square tube layout. Figure 3(a) shows the direction options available for square or rotated square tube layouts*. Figure 3(b) shows how the boundary segmengs are defined using bracketed number pairs to specify the direction and number of tube spaces for a given boundary segment.

* For triangular layouts the angles for direction 2, 4, 6, 8 are, respectively 60^o, -60^o, -120^o, and 120^o while for a rotated triangular layout they are: 30^o, -30^o, -150^o, and 150^o, respectively.

3. Once all bundles are prescribed, define a fine uniform grid*.

4. For each bundle section in turn, "march", in small vector increments, along each boundary line segment. In so doing, identify the fine grid control volumes crossed by a line segment. Assign these "boundary control volumes" a weighting factor of ½.

5. Determine whether the nearest positive I-direction control volume to a boundary control volume is inside or outside the bundle section of interest. If it has not already been assigned, assign it a value of 1 if it is inside and -1 if it is outside.

6. Once all bundle sections are covered by repeated application of steps 4 and 5 identify all inside scalar control volumes using the information from step 5. Assign each of these a weighting factor of 1.

7. Superimpose the working non-uniform coarse grid on the uniform fine grid.

8. Using the information generated in steps 4 to 6 in a summation process, approximate the tube-filled fraction, F, of each coarse-grid scalar control volume. This is illustrated in Figure 4. Calculate the porosity from the linear expression:

$$\beta = 1 + F(\beta_t - 1) \qquad (11)$$

Figure 5 shows how the porosity distribution is defined for a group of hypothetical tube bundles. The triangular symbols located within a scalar control volume (bounded by the solid grid lines) indicate the control volume is completely filled with tubes while the numerical values inside boundary control volumes designate the percent of each control volume filled with tubes.

* The fine grid can be either polar or cartesian depending on the coarse non-uniform grid used to solve the finite control volume equations. The grid spacing in the fine grid can be up to an order of magnitude less than for the coarse grid.

5. FLOW-BLOCKAGE RESISTANCES

As mentioned in Section 2, the local effects of devices such as sealing strips, sealing rods, impingement plates and condensate drain trays are accounted for by treating them as orifices with characteristic loss coefficients varying in value from zero to infinity. The accurate determination of these coefficients depends on how well a blockage device, having an arbitrary orientation with respect to the working grid, can be resolved into a series of orthogonal segments lying across u and v momentum control volumes. The following is an outline of the algorithm developed to calculate the coefficients $k_{u,bl}$ and $k_{v,bl}$:

1. From engineering drawings and/or specification sheets identify all flow blockage devices in the design of interest.

2. Characterize each by specifying (a) four sets of coordinates (Figure 6), and, (b) the coefficient k_{sl} based on a representative area ratio for the device (i.e., see Figure 1). The coordinates PSS1 to PSS4 define the blockage device consisting of the three segments SS1 to SS3; SS1 and SS3 are assumed to be porous with a loss coefficient of k_{sl} while SS2 is assumed to be solid with a loss coefficient of infinity. In theory, it is possible to model any type of flow blockage by varying the lengths of the component segments of a single device or by combining two or more blockage devices.

3. For each blockage device in turn, starting at the origin of each segment, march along it in steps using an incremental vector*.

* The incremental vector has the same direction as the segment and a length equal to 1/100 of a representation grid spacing.

4. After each step, check to see if the nearest u and v control volumes are partially or entirely blocked by the segment. If the segment passes through these control volumes, determine the local gap widths and calculate the corresponding loss coefficients using equation (9). Typical examples of several local gaps widths seen by a u-momentum control volume based on a polar grid are illustrated in Figure 7.

Examples of how flow blockage devices of various orientations are represented on a polar grid are illustrated in Figures 8(a) and 8(b). Each device is defined as a series of orthogonal segments across u and v momentum control volumes. Non-zero loss coefficients are calculated only for control volumes crossed by these segments. The Figures clearly show how the finer grid results in a more faithful representation of the true orientations of the blocking devices.

6. COMPUTATION OF ISOTHERMAL FLOWS

Several cases were run to compute isothermal flow fields for various tube-bundle and blocking device configurations. All computations were done with the effective viscosity set to the laminar value so that the only effective momentum sinks were the hydraulic resistance terms. In all cases, satisfactory convergence was obtained within about 50 iterations. The time taken per iteration, using 1700 internal node points, was 1.7 seconds on a CDC CYBER 170 Model 175 computer.

Figure 9 illustrates the predicted velocity field for a heat exchanger with a drilled impingement plate across the inlet. The direction and length of the arrows represent the vector sum of u and v velocities at each node point.

Figures 10(a) and 10(b) show the calculated velocity vector field and normalized pressure contours predicted for a non-symmetric four-bundle heat exchanger. The real blockage devices are large diameter tubes modelled as straight line segments having lengths equal to the tube diameter. Figure 10(a) shows the effectiveness of the centre tubes in diverting flow back into the tube bundles. As expected, the highest velocities are predicted to occur on either side of the flow blocking tubes. Tubes in this area could be susceptible to flow-induced vibration damage.

An illustration of the predicted flow distribution in a power plant condenser tube-bundle configuration is shown in Figure 11. Since the computation was done merely to illustrate the generality of the algorithms, the imposed inlet and outlet flow conditions are hypothetical.

7. CONCLUDING REMARKS

A computational procedure has been developed to model the 2-dimensional isothermal flow in the cross-sectional plane of circular or rectangular shell-and-tube heat exchangers with tube bundles of arbitrary boundaries and flow blocking devices of arbitrary orientation and location. The modelling approach is sufficiently robust and general that it can be extended to calculate diabatic flows in two-and-three dimensions without much difficulty. However, because predictions depend heavily on empirical fluid-flow correlations, it is important to validate the computational method against experimental data before results can be used to make quantitative assessments of proposed or operating heat exchanger designs.

ACKNOWLEDGEMENTS

This work was partially funded by HTFS; their support is gratefully acknowledged. Thanks are also due to Mrs. M. Tremblay for typing this manuscript.

REFERENCES

[1] CARVER, M.B., CARLUCCI, L.N., INCH, W.W.R., "Thermal-Hydraulics in Recirculating Steam Generators - THIRST Code User's Manual", Atomic Energy of Canada Limited Report, AECL-7254, April 1981.

[2] CARLUCCI, L.N., SUTHERLAND, D., "The Effects of Various Empirical Correlations on the Predictions of a Steam Generator Thermal-Hydraulics Code", ASME Paper 81-WA/NE-5, 1981.

[3] SINGHAL, A.K., KEETON, L.W., SPALDING, D.B., "Predictions of Thermal-Hydraulics of a PWR Steam Generator by using the Homogeneous and Two-Slip Flow Models", Paper presented at the 19th National Heat Transfer Conference held in Orlando, Florida, July 27-30, 1980.

[4] OLIVE, J., "Simulation of Three-Dimensional Two-Phase Flow in a PWR Steam Generator", Paper presented at European Two-Phase Flow Group Meeting held in Paris, France, June 2-4, 1982.

[5] Butterworth, D., "The Correlation of Cross-Flow Data by Means of the Permeability Concept", United Kingdom Atomic Energy Authority Report AERE-R-9435, April 1979.

[6] PATANKAR, S.V., Numerical Heat Transfer and Fluid Flow, Hemisphere Publishing Corp., 1980.

[7] GOSMAN, A.D., PUN, W.M., Lecture Notes for Course Titled, "Calculation of Recirculating Flows", Imperial College, HTS/74/2, 1974.

ILLUSTRATIONS

Figure 1: Illustration of Representative Areas Required to Characterize a Sealing Strip as an Orifice.

Figure 2: Illustration of Scalar and Vector Control Volumes used in Staggered Grid Concept.

Figure 3: Example of Tube-Bundle Definition for a Square Tube Layout: (a) 8 Possible Principal Directions, (b) Definition of Boundary Segment Specification, i.e., (5,4) = (direction number, number of tube spaces).

Figure 4: Example Porosity Definition using Coarse Working Grid Superimposed on Fine Uniform Grid.

Figure 5: Example of Definition of Hypothetical Multiple Bundles; Solid Grid Lines are Control Volumes Surfaces. Triangles Indicate Entirely Tube-Filled, Numerical Values Indicate Estimated Per Cent Tube-Filled.

Figure 6: Definition of Flow Blockage Device in Terms of Coordinates PSS1 to PSS4 and Segment Lengths SS1 to SS3.

Figure 7: Examples of Various Partial Blockage Configurations and Corresponding Local Gap Areas for u-Velocity Control Volume. These are only for Segments SS2 and SS3.

Figure 8: Examples of How the Same Flow Blockage Devices are Resolved by (a) A Relatively Fine Working Grid, and (b) a Coarse Working Grid.

Figure 9: Computed Isothermal Velocity Distributions for an Actual Configuration Consisting of One Drilled Impingement Plate, Four Sealing Strips and One Tube Bundle.

Figure 10: Computed Isothermal (a) Velocity, and (b) Normalized Pressure Fields for an Actual Configuration Consisting of Four Asymmetric Tube Bundles and Six Sealing Rods.

Figure 11: Computed Isothermal Velocity Field in a Power Plant Condenser Configuration Consisting of Two Tube Bundles and Two Condensate Drain Trays. Flow Conditions at Boundaries are Hypothetical.

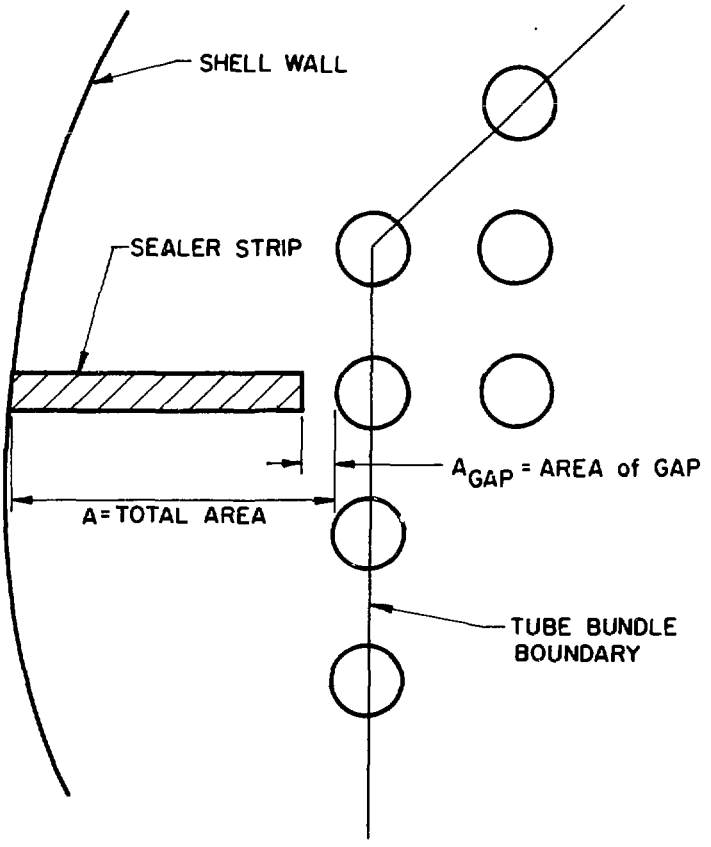

Figure 1: Illustration of Representative Areas Required to Characterize a Sealing Strip as an Orifice.

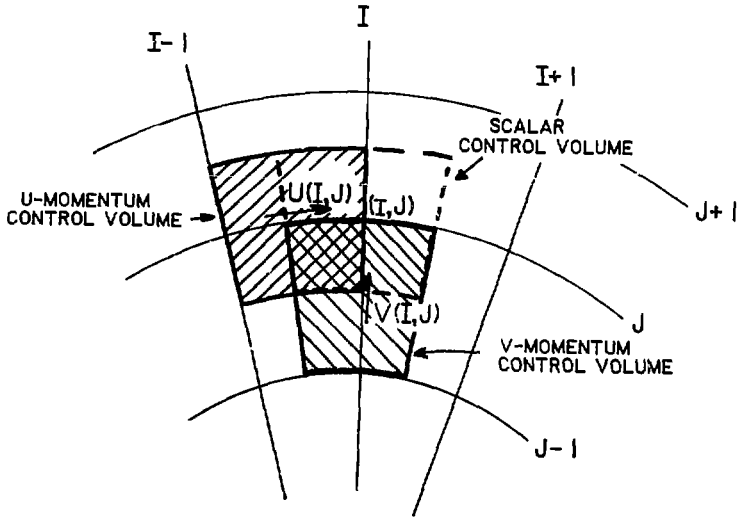

Figure 2: Illustration of Scalar and Vector Control Volumes used in Staggered Grid Concept.

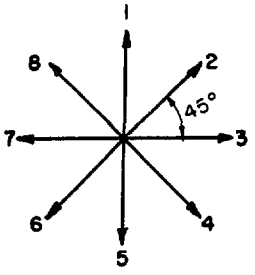

SQUARE & ROTATED SQ.

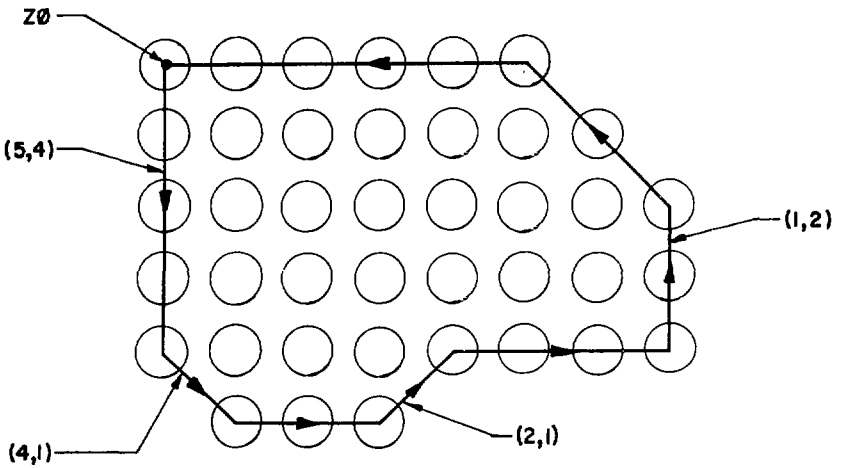

(DIRECTION NO: , NO: of TUBE SPACES)

Figure 3: Example of Tube-Bundle Definition for a Square Tube Layout: (a) 8 Possible Principal Directions, (b) Definition of Boundary Segment Specification, i.e., (5,4) = (direction number, number of tube spaces).

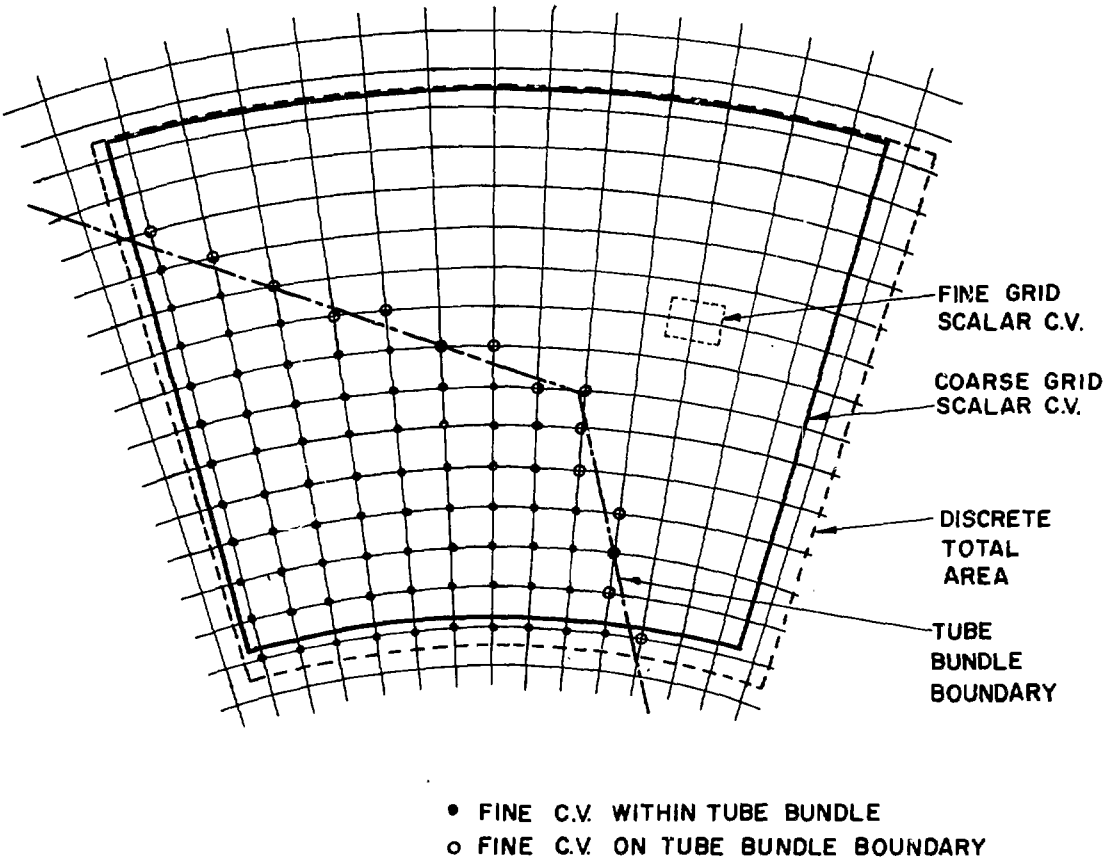

Figure 4: Example Porosity Definition using Coarse Working Grid Superimposed on Fine Uniform Grid.

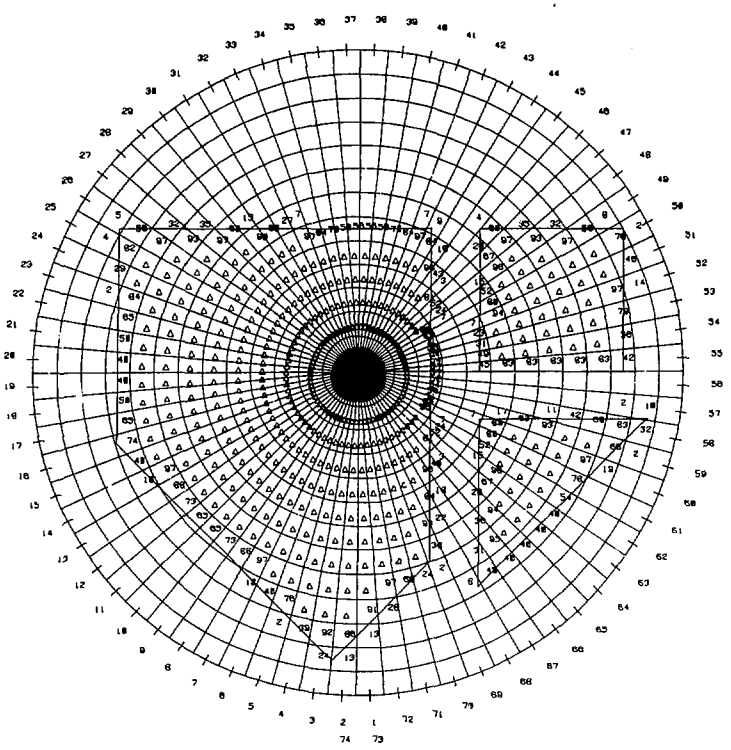

Figure 5: Example of Definition of Hypothetical Multiple Bundles; Solid Grid Lines are Control Volumes Surfaces. Triangles Indicate Entirely Tube Filled, Numerical Values Indicate Estimated Per Cent Tube-Filled.

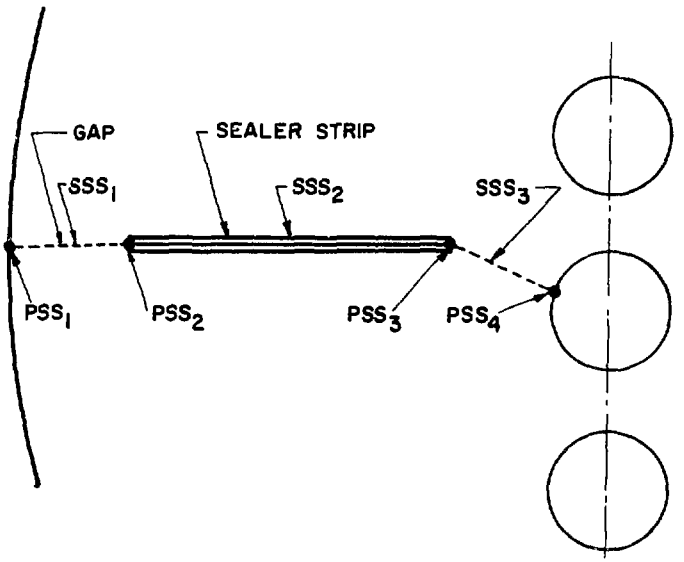

Figure 6: Definition of Flow Blockage Device in Terms of Coordinates PSS1 to PSS4 and Segment Lengths SS1 to SS3.

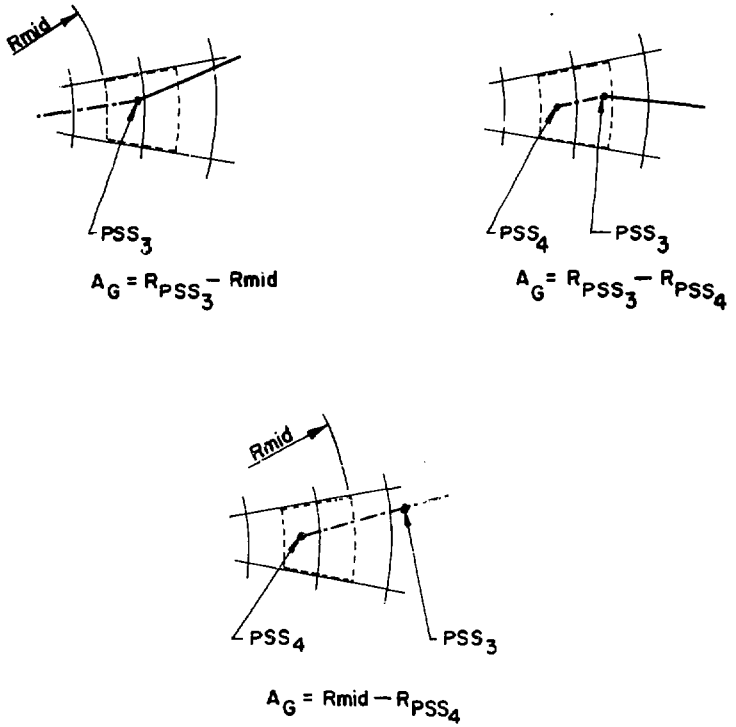

Figure 7: Examples of Various Partial Blockage Configurations and Corresponding Local Gap Areas for u-Velocity Control Volume. These ar only for Segments SS2 and SS3.

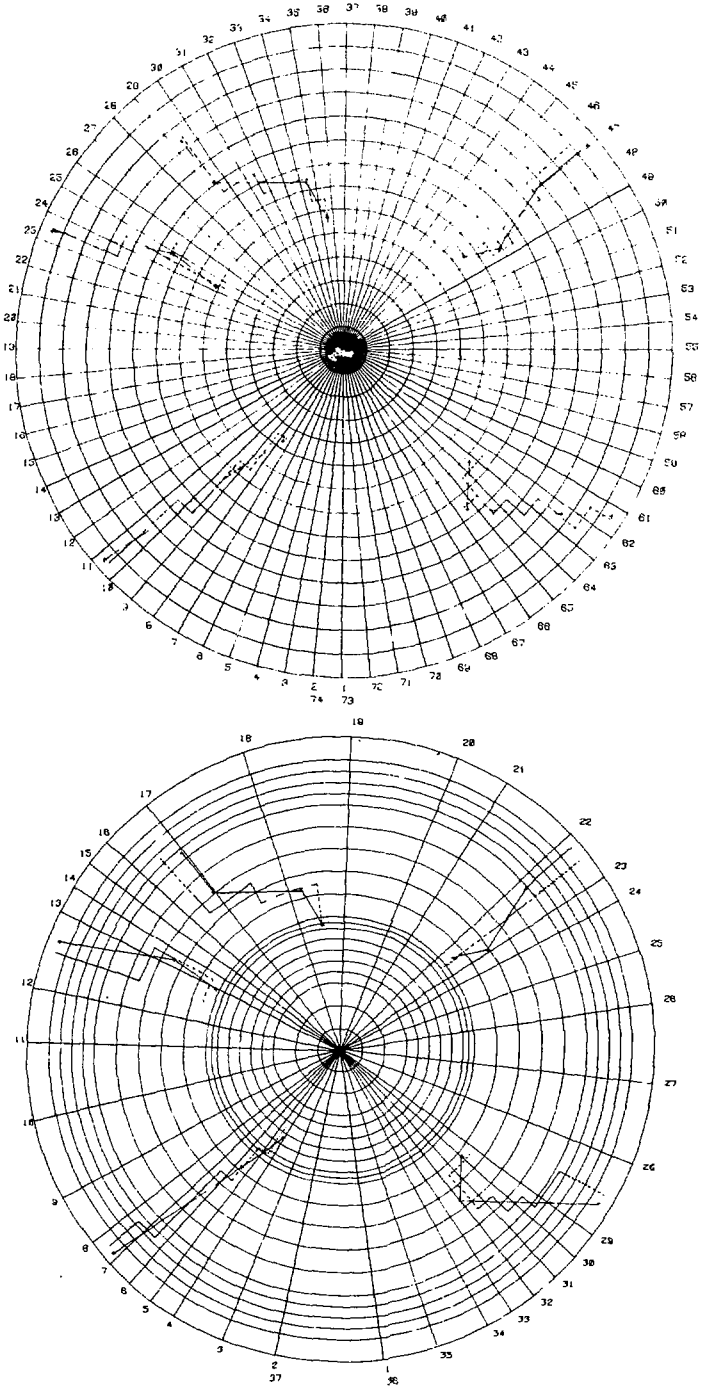

Figure 8: Examples of How the Same Flow Blockage Devices are Resolved by (a) A Relatively Fine Working Grid, and (b) a Coarse Working Grid.

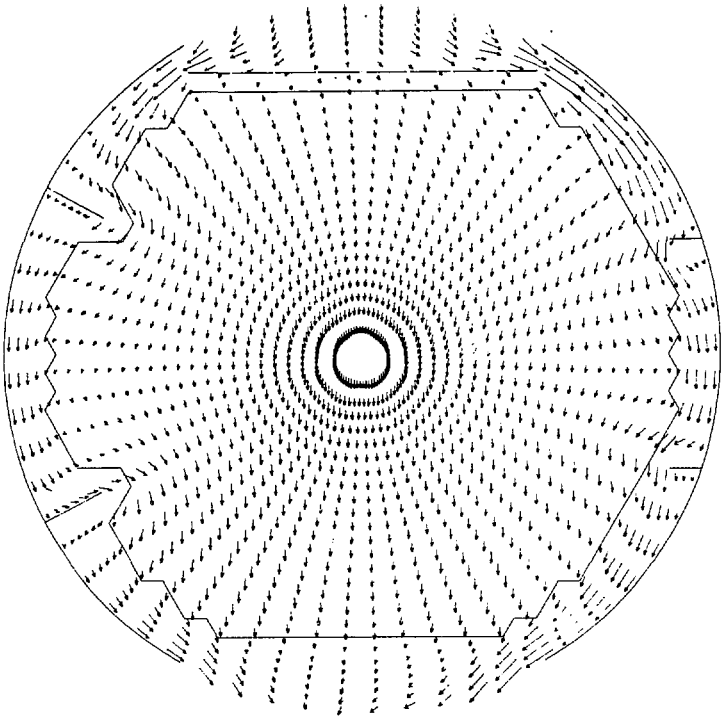

Figure 9: Computed Isothermal Velocity Distributions for an Actual Configuration Consisting of One Drilled Impingement Plate, Four Sealing Strips and One Tube Bundle.

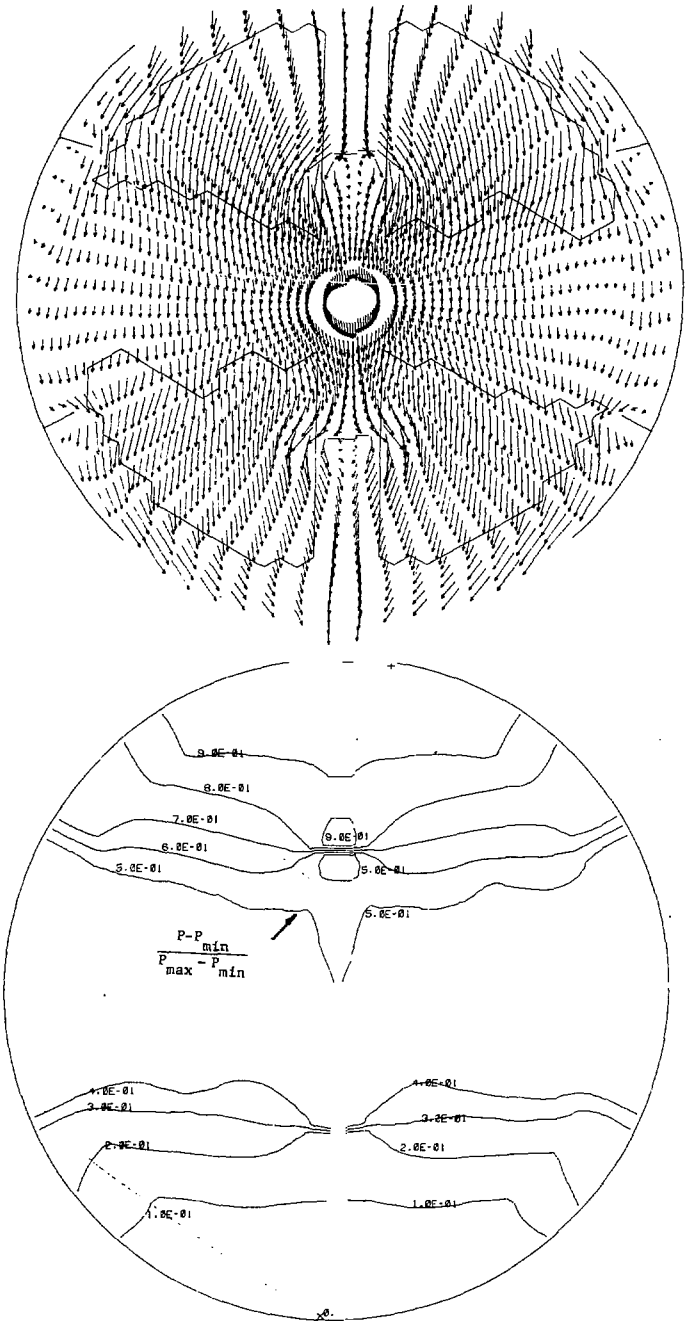

Figure 10: Computer Isothermal (a) Velocity, and (b) Normalized Pressure Fields for an Actual Configuration Consisting of Four Asymmetric Tube Bundles and Six Sealing Rods.

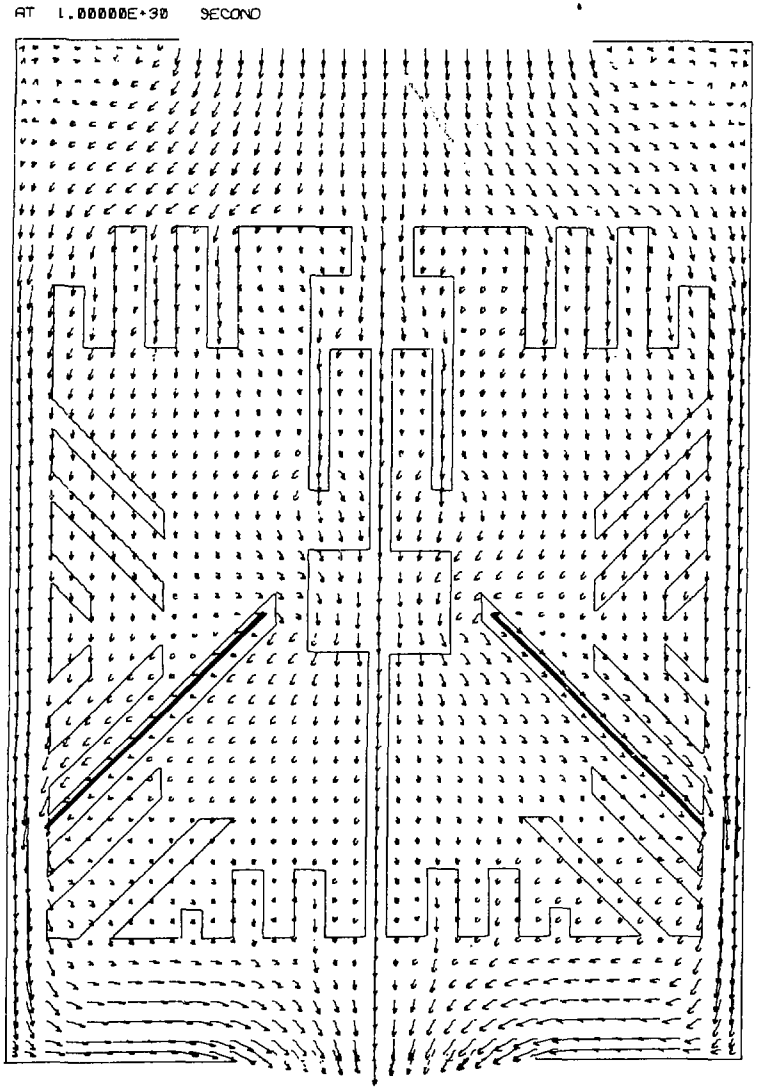

Figure 11: Computed Isothermal Velocity Field in a Power Plant Condenser Configuration Consisting of Two Tube Bundles and Two Condensate Drain Trays. Flow Conditions at Boundaries are Hypothetical.

ISSN 0067 - 0367

To identify individual documents in the series we have assigned an AECL- number to each.

Please refer to the AECL- number when requesting additional copies of this document

from

Scientific Document Distribution Office
Atomic Energy of Canada Limited
Chalk River, Ontario, Canada
K0J 1J0

Price $2.00 per copy

ISSN 0067 - 0367

Pour identifier les rapports individuels faisant partie de cette série nous avons assigné un numéro AECL- à chacun.

Veuillez faire mention du numéro AECL- si vous demandez d'autres exemplaires de ce rapport

au

Service de Distribution des Documents Officiels
L'Energie Atomique du Canada Limitée
Chalk River, Ontario, Canada
K0J 1J0

Prix $2.00 par exemplaire

2400–83